arXiv:cond-mat/0411517v1 [cond-mat.other] 19 Nov 2004

Shape resonances for ultracold atom gases in carbon nanotube waveguides

V. Peano, M. Thorwart, C. Mora, and R. Egger
Institut für Theoretische Physik, Heinrich-Heine-Universität, D-40225 Düsseldorf, Germany
(Dated: February 2, 2008)

We propose an experimentally viable setup for the realization of one-dimensional ultracold atom gases in a nanoscale magnetic waveguide formed by two doubly-clamped suspended carbon nanotubes. All common decoherence and atom loss mechanisms are shown to be small. We discuss general consequences of a non-parabolic confinement potential, in particular novel two-body shape resonances, which could be observed in this trap.

PACS numbers: 03.65.Nk, 03.75.Gg, 73.63.Fg

The ongoing progress in the fabrication and manipulation of micro- or nanoscale structures has recently allowed for systematic studies of ultracold atom gases, where current-carrying wires generate magnetic fields trapping neutral atoms ('atom chips') [1, 2]. For instance, the Bose-Einstein condensation (BEC) of microchip-confined atoms has been successfully demonstrated by several groups [3]. Such an approach is particularly promising in the context of integrated atomic matter-wave interferometry and optics [4], and combines the strengths of nanotechnology and atomic physics. So far, decoherence and atom loss constitute central impediments, since atoms are relatively close to 'hot' macroscopic surfaces or current-carrying wires (with typical diameters of several μm), where the Casimir-Polder potential and Johnson noise can seriously affect stability [5, 6, 7]. To reduce these effects, further miniaturization would be desirable. While at first sight this goal conflicts with the requirement of large currents forming the trapping potentials, we propose that when using suspended carbon nanotubes (NTs) [8] (with diameters of a few nm) as wires, nanoscale atom chip devices basically free of decoherence or atom loss can be built with state-of-the-art technology. With relevant length scales below optical and cold-atom de Broglie wavelengths, this also paves the way for the observation of interesting and largely unexplored many-body physics in one dimension (1D) [9], involving either bosons or fermions. Examples include the interference properties of interacting matter waves [10], spin-charge separation [11], fractional statistics and atom number fractionalization [12], and the 1D analogue of the BEC-BCS crossover [13]. Previous realizations of 1D cold atoms were reported using optical lattices [14, 15, 16] and magnetic traps [17], but they involve arrays of 1D or elongated 3D systems, where the above many-body effects are difficult to observe. Our proposal completely eliminates unwanted substrate effects and implies a drastically reduced transverse size (a few nm) of the cloud. Hence rather high atom densities could be achieved, allowing for stable operation and sensible optical detection schemes.

The proposed nanoscale waveguide confining ultracold atoms to 1D is sketched in Fig. 1. The setup employs two suspended doubly-clamped NTs, where nanofabrication techniques routinely allow for trenches with typical depth and length of several μm [8]. To minimize decoherence and loss effects [6], the substrate should be insulating apart from thin metal strips to electrically contact the NTs. Since strong currents in the mA-regime are necessary, thick multiwall nanotubes (MWNTs) or 'ropes' (bundles) [8] are best suited. Due to the suspended geometry, the disturbing influence of the substrate is largely eliminated, and employing an additional longitudinal magnetic field to eliminate Majorana spin flips [18, 19], neutral atoms in a weak-field seeking state can be trapped between the NTs. Studying various sources for decoherence, heating or atom loss, and estimating the related time scales, we find that, for reasonable parameters, detrimental effects are small. We also analyze effects due to the non-parabolicity of the transverse trap potential, which is inevitable in all common traps but particularly pronounced in the present case. We find many two-body shape resonances, which allow to tune atom-atom interactions similar to standard Feshbach resonances. Previous work has only studied parabolic traps, where center-of-mass (COM) variables decouple. Then incoming scattering waves can visit only one out of many bound states normally available, leading to a single 'confinement-induced resonance' [20]. Here we solve the two-body problem for general transverse confinement, and then apply the results to the proposed trap. As a concrete example, we shall consider ^{87}Rb atoms in the weak-field seeking hyperfine state $|F, m_F\rangle = |2, 2\rangle$.

We next describe the setup in Fig. 1 in detail, where the same (homogeneous) current I flows through the two NTs at $(\pm x_0, 0, z)$, and a magnetic field B_z is applied along the z-direction. Neglecting boundary effects due to the finite tube length L, the magnetic field at position $\mathbf{x} = (x, y, z) = (\mathbf{x}_\perp, z)$ is

$$\mathbf{B}(\mathbf{x}) = \frac{\mu_0 I}{2\pi} \frac{1}{[(x-x_0)^2+y^2][(x+x_0)^2+y^2]} \times \begin{pmatrix} -2y(x^2+x_0^2+y^2) \\ 2x(x^2+y^2-x_0^2) \\ 0 \end{pmatrix} + \begin{pmatrix} 0 \\ 0 \\ B_z \end{pmatrix}$$

with the vacuum permeability μ_0. The transverse con-

finement potential is $V(\mathbf{x}_\perp) = \mu|\mathbf{B}(\mathbf{x})|$, where $\mu = m_F g_F \mu_B$ with the Landé factor g_F and the Bohr magneton μ_B. Under the adiabatic approximation [18], m_F is a constant of motion, and the potential is harmonic very close to the minimum of the trap, with frequency $\omega = [\mu/(mB_z)]^{1/2}\mu_0 I/(\pi x_0^2)$ and associated transverse confinement length $a_\perp = (\hbar/m\omega)^{1/2} \ll x_0$, where m is the atom mass. The adiabatic approximation is valid as long as $\omega \ll \omega_L$ with the Larmor frequency $\omega_L = \mu B_z/\hbar$. Trapped atoms can in general also make non-adiabatic Majorana spin flips to a strong-field seeking state, and thereby escape from the trap [1, 19]. The associated loss rate is $\Gamma \simeq (\pi\omega/2)\exp(1-1/\chi)$ with $\chi = \hbar\omega/(\mu B_z)$ [18]. For convenience, we switch to a dimensionless form of the full potential $V(\mathbf{x}_\perp)$ by measuring energies in units of $\hbar\omega$ and lengths in units of $a_\perp$,

$$\chi V = \left(1 + \chi d^4 \frac{(x^2+y^2)[(x^2+y^2+d^2)^2 - 4x^2d^2]}{[(x-d)^2+y^2]^2[(x+d)^2+y^2]^2}\right)^{1/2}, \tag{1}$$

which depends only on $d = x_0/a_\perp$ and χ. To give an example, we take $I = 1$ mA, representing a reasonable current through thick MWNTs [8]. For $d = 10$ and $\Gamma/\omega = 10^{-6}$ ($\chi = 0.067$), we obtain $B_z = 20$ G, $x_0 = 79$ nm and $\omega = 2\pi \times 1.85$ MHz, corresponding to a very tight trap. The potential is shown for these parameters in Fig. 2 [21].

For stable operation, it is essential that destructive effects like atom loss, heating or decoherence are small. One loss process proceeds via (i) non-adiabatic Majorana spin flips as discussed above. Another one is (ii) atom loss due to tunneling out of the trap. The WKB tunneling rate γ_t can be estimated easily for an atom in the transverse ground state escaping along the least-confined y-direction, see Fig. 2,

$$\gamma_t/\omega \simeq (2\pi)^{-1}\exp\left[-2\sqrt{2}\int_{y_1}^{y_2} dy[V(0,y)-1]^{1/2}\right].$$

For the above parameters, we find numerically $y_1 = 1.47, y_2 = 68.09$, and hence $\gamma_t/\omega \approx 10^{-100}$. Atom loss may also originate from (iii) noise-induced spin flips, where current fluctuations cause a fluctuating magnetic field generating the Majorana spin flip rate [5]

$$\gamma_{sf} \simeq \left(\frac{\mu_0\mu}{2\pi\hbar x_0}\right)^2 \frac{S_I(\omega_L)}{2},\ S_I(\omega) = \int dt e^{-i\omega t}\langle I(t)I(0)\rangle.$$

At room temperature and for typical voltages $V_0 \approx 1$ V, we have $\hbar\omega_L \ll k_BT \ll eV_0$, and $S_I(\omega_L)$ is expected to equal the shot noise $2eI/3$ of a diffusive wire. For the parameters above, a rather small escape rate results, $\gamma_{sf} \approx 0.017$ Hz. Next we study (iv) the transverse NT deflection due to their mutual magnetic repulsion, using a standard elasticity model for a doubly clamped wire in the limit of small deflections [23]. For small NT displacements $\phi(z)$, the equation of motion is $\rho_L\ddot{\phi} = -YM_I\phi'''' + \mu_0 I^2/(4\pi x_0)$, where ρ_L is the linear mass density, Y is Young's modulus and M_I the NT's moment of inertia. The static solution under the boundary conditions $\phi(0,L) = \phi'(0,L) = 0$ is $\phi(z) = \mu_0[Iz(z-L)]^2/(96\pi YM_I x_0)$. Using typical material parameters from Ref. [8], the maximum displacement is $\phi(L/2) \approx 0.08$nm for $L = 10\mu$m. Hence the mutual magnetic repulsion of the NTs is weak. (v) Thermal NT vibrations might create decoherence and heating, and could even cause a transition to the first excited state of the trap. The maximum mean square displacement is $\sigma^2 = \langle\phi^2(L/2)\rangle = k_BTL^3/(192YM_I)$ [23], which for the above parameters gives $\sigma \approx 0.2$ nm at room temperature. This is much smaller than the transverse size $a_\perp$ of the atomic cloud. Detailed analysis shows that the related decoherence rate is also negligible. Another decoherence mechanism comes from (vi) current fluctuations in the NTs. Following the analysis of Ref. [7], the corresponding decoherence rate can be estimated for the above parameters as $\gamma_c/\omega < 10^{-7}$. We conclude that no serious decoherence, heating or loss mechanisms are expected for reasonable parameters of this nanotrap.

Next we discuss s-wave atom-atom interactions in this trap. We assume that the 3D interaction can be described by a Fermi pseudopotential [24] via the 3D scattering length a. To keep generality, let us investigate two-body scattering for arbitrary confining potential $V(\mathbf{x}_\perp)$, and later specialize to Eq. (1). Unlike for a harmonic trap, the problem does *not* decouple when formulated in terms of the COM coordinate $\mathbf{R} = (\mathbf{x}_1+\mathbf{x}_2)/2 = (\mathbf{R}_\perp, Z)$ and the relative coordinate $\mathbf{r} = \mathbf{x}_2 - \mathbf{x}_1 = (\mathbf{r}_\perp, z)$. Following standard steps [9], the pseudopotential is enforced as a boundary condition for the two-particle wavefunction,

$$\Psi(\mathbf{R}, \mathbf{r}\to 0) = \frac{f(\mathbf{R})}{4\pi|\mathbf{r}|}(1-|\mathbf{r}|/a). \tag{2}$$

Without loss of generality, we set the longitudinal COM momentum to zero such that Z drops out. Furthermore, we can put $\mathbf{r}_\perp = 0$ and then let $z \to 0$ in Eq. (2). The solution of the two-particle Schrödinger equation $\Psi(\mathbf{R}_\perp, z)$ then takes the general form

$$\Psi(\mathbf{R}_\perp, z) = \Psi_0(\mathbf{R}_\perp, z) + \int d\mathbf{R}'_\perp G_E(\mathbf{R}_\perp, z; \mathbf{R}'_\perp, 0)\frac{f(\mathbf{R}'_\perp)}{m}. \tag{3}$$

For $\Psi_0 = 0$, this leads to bound-state solutions with energy $E < 2E_0$ discussed elsewhere [25], where E_0 is the single-particle ground-state energy. Here we focus on scattering solutions at low energies E slightly above $2E_0$, where exactly one transverse channel is open. Then $\Psi_0(\mathbf{R}_\perp, z) = e^{ikz}\psi_0^2(\mathbf{R}_\perp)$ describes two incoming atoms with (small) relative longitudinal momentum $\hbar k = \sqrt{2m(E-2E_0)}$ in the (transverse) single-particle state $\psi_0(\mathbf{R}_\perp)$ with energy E_0. Some algebra yields the

two-particle Green's function

$$G_E(\mathbf{R}_\perp, z; \mathbf{R}'_\perp, 0) = \psi_0^2(\mathbf{R}_\perp)\bar{\psi}_0^2(\mathbf{R}'_\perp)\frac{im}{2k}e^{ik|z|} + \int_0^\infty dt\, e^{Et}\sqrt{\frac{m}{4\pi t}}e^{-z^2m/4t}\tilde{G}_t(\mathbf{R}_\perp, \mathbf{R}'_\perp), \quad (4)$$

where the bar denotes complex conjugation, and

$$\tilde{G}_t(\mathbf{R}_\perp, \mathbf{R}'_\perp) = [G_t^{(0)}]^2 - e^{-2E_0 t}\psi_0^2(\mathbf{R}_\perp)\bar{\psi}_0^2(\mathbf{R}'_\perp),$$
$$G_t^{(0)}(\mathbf{R}_\perp, \mathbf{R}'_\perp) = \sum_\lambda e^{-E_\lambda t}\psi_\lambda(\mathbf{R}_\perp)\bar{\psi}_\lambda(\mathbf{R}'_\perp).$$

Here, $G_t^{(0)}$ is the (transverse) single-particle Green's function, with single-particle states ψ_λ and energy E_λ, and the two-particle Green's function $\tilde{G}_t$ acts on the Hilbert space $\mathcal{H}_{\rm closed}$, orthogonal to the open channel. Inserting Eq. (4) into Eq. (3) yields for $|z| \to \infty$ a standard scattering solution $\Psi(\mathbf{R}, z) = \psi_0^2(\mathbf{R}_\perp)(e^{ikz} + f_e(k)e^{ik|z|})$ with scattering amplitude

$$f_e(k) = \frac{i}{2k}\int d\mathbf{R}'_\perp \bar{\psi}_0^2(\mathbf{R}'_\perp)f(\mathbf{R}'_\perp). \quad (5)$$

Enforcing Eq. (2) then leads to an integral equation,

$$-\frac{f(\mathbf{R}_\perp)}{4\pi a} = \int d\mathbf{R}'_\perp \zeta_E(\mathbf{R}_\perp, \mathbf{R}'_\perp)f(\mathbf{R}'_\perp) + \psi_0^2(\mathbf{R}_\perp) + \frac{i\psi_0^2(\mathbf{R}_\perp)}{2k}\int d\mathbf{R}'_\perp \bar{\psi}_0^2(\mathbf{R}'_\perp)f(\mathbf{R}'_\perp), \quad (6)$$

where the singular behavior has been split off by introducing a regularized kernel in $\mathcal{H}_{\rm closed}$,

$$\zeta_E = \int_0^\infty \frac{dt}{\sqrt{4\pi m t}}\left(e^{Et}\tilde{G}_t(\mathbf{R}_\perp, \mathbf{R}'_\perp) - \frac{m}{4\pi t}\delta(\mathbf{R}_\perp - \mathbf{R}'_\perp)\right).$$

The integral equation (6) is most conveniently solved by expansion in a suitable orthonormal basis $|j\rangle$,

$$|f\rangle = \sum_j f_j|j\rangle, \quad f_j = \int d\mathbf{R}_\perp \langle j|\mathbf{R}_\perp\rangle f(\mathbf{R}_\perp), \quad (7)$$

where $|0\rangle$ corresponds to $\langle \mathbf{R}_\perp|0\rangle = c\psi_0^2(\mathbf{R}_\perp)$ with normalization constant c. Thereby we can express Eq. (6) in compact notation,

$$-\frac{|f\rangle}{4\pi a} = \frac{|0\rangle}{c} + \frac{i}{2k}\frac{|0\rangle}{c^2}\langle 0|f\rangle + \zeta_E|f\rangle, \quad (8)$$

which is solved by

$$|f\rangle = \frac{-1/c}{1 - i/(ka_{\rm 1D})}\left(\zeta_E + \frac{1}{4\pi a}\right)^{-1}|0\rangle. \quad (9)$$

Here, the parameter $a_{\rm 1D}$ follows in the form

$$a_{\rm 1D} = -\frac{2c^2}{\langle 0|[\zeta_E + 1/(4\pi a)]^{-1}|0\rangle}. \quad (10)$$

Since $f_e(k) = -1/(1 + ika_{\rm 1D})$ follows from Eq. (5), $a_{\rm 1D}$ can be identified with the *1D scattering length*. The effective 1D atom-atom interaction potential is then $V_{\rm 1D}(z, z') = g_{\rm 1D}\delta(z - z')$ with interaction strength $g_{\rm 1D} = -2\hbar^2/(ma_{\rm 1D})$ [9, 20]. For very low energies, $k \to 0$, we can now put $E = 2E_0$ in Eq. (10). For a binding trap, ζ_{2E_0} is an Hermitian operator with discrete spectrum $\{\lambda_n\}$ and eigenvectors $|e_n\rangle$, and hence we find

$$a_{\rm 1D}^{-1} = -\frac{1}{2c^2}\sum_n \frac{|\langle 0|e_n\rangle|^2}{\lambda_n + 1/(4\pi a)}. \quad (11)$$

Let us then denote $H_{\rm closed}$ as the projection of the Hamiltonian to $\mathcal{H}_{\rm closed}$. The boundary condition for the corresponding bound state is enforced by $-|f\rangle/(4\pi a) = \zeta_E|f\rangle$. Thus, for $a = -(4\pi\lambda_n)^{-1}$, a bound state of $H_{\rm closed}$ with energy $E = 2E_0$ exists, fulfilling Eq. (2) with $f(\mathbf{R}) = \langle \mathbf{R}_\perp|e_n\rangle$. In agreement with general arguments [20, 26], provided $\langle 0|e_n\rangle \neq 0$, a bound state of $H_{\rm closed}$ at $a = -(4\pi\lambda_n)^{-1}$ corresponds to a *shape resonance* in the 1D interaction strength $g_{\rm 1D}$.

The two-body problem can thereby be solved numerically for any given confinement potential by diagonalizing ζ_{2E_0}. We note in passing that for certain potentials, including a hard-box confinement, Eq. (11) can also be computed analytically in closed form [25]. In general, every eigenvalue λ_n corresponds to a different shape resonance, unless the overlap $\langle 0|e_n\rangle$ vanishes due to some underlying symmetry. For a parabolic confinement, the decoupling of the COM motion implies that only one resonance is permitted, and some algebra gives indeed from Eq. (11) the known result $a_{\rm 1D} = -(a_\perp^2/a)(1 - 1.0326a/a_\perp)$ [20]. For a general confinement, there are in principle infinitely many resonances. In practice, however, only few of them can be resolved since most of them appear at $a/a_\perp \to 0$. In addition, most resonances are extremely sharp and will therefore be hard to detect. The 1D interaction strength $g_{\rm 1D}$ for the potential (1) in the case of ^{87}Rb atoms is shown in Fig. 3 as a function of the NT current I. At least two different shape resonances are predicted to be observable for realistic and discernible values of I in the mA regime. These resonances could be used to tune the strength and the sign of the two-body interactions by simply adjusting the NT current.

To conclude, we propose a nanoscale waveguide for ultracold atoms based on doubly clamped suspended nanotubes. All common sources of imperfection can be made sufficiently small to enable stable operation of the setup. Detection certainly constitutes an experimental challenge in this truly 1D limit. However, we note that single-atom detection schemes are currently being developed, which would also allow to probe the tight 1D cloud here, e.g., by combining cavity quantum electrodynamics with chip technology [2], or by using additional perpendicular wires/tubes 'partitioning' the atom cloud [22]. This

may then allow to study interesting many-body physics in 1D in an unprecedented manner. Atom-atom interactions can be tuned by shape resonances, which we have described for arbitrary transverse confinement.

We thank A. Görlitz and A.O. Gogolin for discussions, and acknowledge support by the SFB/TR 12.

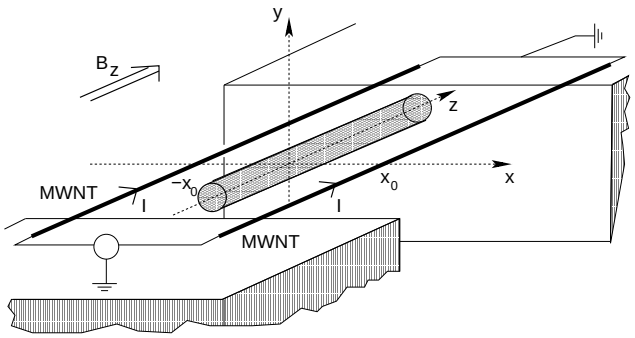

FIG. 1: Sketch of the proposed device. The two current-carrying suspended NTs are positioned at $(\pm x_0, 0, z)$. The shaded region indicates the atom gas.

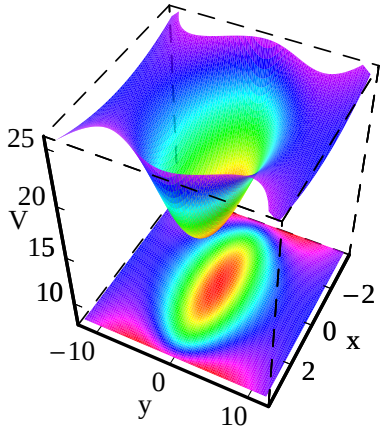

FIG. 2: (Color online) Transverse trapping potential of the nanoscale waveguide, see text.

[1] R. Folman, P. Krüger, J. Schmiedmayer, J. Denschlag, and C. Henkel, Adv. At. Mol. Opt. Phys. **48**, 263 (2002).
[2] J. Reichel, Appl. Phys. B **75**, 469 (2002).
[3] H. Ott, J. Fortagh, G. Schlotterbeck, A. Grossmann, and C. Zimmermann, Phys. Rev. Lett. **87**, 230401 (2001); W. Hänsel, P. Hommelhoff, T.W. Hänsch, and J. Reichel, Nature **413**, 498 (2001); A. Leanhardt *et al.*, Phys. Rev. Lett. **90**, 100404 (2003).
[4] M.A. Kasevich, Science **298**, 136 (2002).
[5] C. Henkel, S. Pötting, and M. Wilkens, Appl. Phys. B **69**, 379 (1999).
[6] Yu-ju Lin, I. Teper, C. Chin, and V. Vuletić, Phys. Rev. Lett. **92**, 050404 (2004).
[7] C. Schroll, W. Belzig, and C. Bruder, Phys. Rev. A **68**, 043618 (2003).
[8] M.S. Dresselhaus, G. Dresselhaus, and Ph. Avouris (eds.), *Carbon Nanotubes* (Berlin, Springer 2001).
[9] D.S. Petrov, D.M. Gangardt, and G.V. Shlyapnikov, J. Phys. IV France **116**, 5 (2004).
[10] S. Chen and R. Egger, Phys. Rev. A **68**, 063605 (2003).
[11] A. Recati, P.O. Fedichev, W. Zwerger, and P. Zoller, Phys. Rev. Lett. **90**, 020401 (2003).
[12] K.-V. Pham, M. Gabay, and P. Lederer, Phys. Rev. B **61**, 16397 (2000).
[13] I.V. Tokatly, Phys. Rev. Lett. **93**, 090405 (2004); J.N. Fuchs, A. Recati, and W. Zwerger, *ibid.* **93**, 090408 (2004); C. Mora, R. Egger, A.O. Gogolin, and A. Komnik, *ibid.* **93**, 170403 (2004).
[14] T. Stöferle, H. Moritz, C. Schori, M. Köhl, and T. Esslinger, Phys. Rev. Lett. **92**, 130403 (2004).
[15] B. Paredes *et al.*, Nature **429**, 277 (2004).
[16] T. Kinoshita, T. Wenger, and D.S. Weiss, Science **305**, 112 (2004).
[17] A. Görlitz *et al.*, Phys. Rev. Lett. **87**, 130402 (2001).
[18] C.V. Sukumar and D.M. Brink, Phys. Rev. A **56**, 2451 (1997).
[19] M.P.A. Jones, C.J. Vale, D. Sahagun, B.V. Hall, and E.A. Hinds, Phys. Rev. Lett. **91**, 080401 (2003).
[20] M. Olshanii, Phys. Rev. Lett. **81**, 938 (1998); T. Bergeman, M.G. Moore, and M. Olshanii, *ibid.* **91**, 163201 (2003).
[21] In order to create a 1D trap, a weak longitudinal confinement should be added, e.g., by means of additional NTs perpendicular to the z-axis (at $y = 0$), see Ref. [22].
[22] J. Reichel and J.H. Thywissen, J. Phys. IV France **116**, 265 (2004).
[23] S. Sapmaz, Ya.M. Blanter, L. Gurevich, and H.S.J. van der Zant, Phys. Rev. B **67**, 235414 (2003).
[24] K. Huang, *Statistical Mechanics* (Wiley, New York, 1987).
[25] V. Peano, M. Thorwart, C. Mora, and R. Egger, in preparation.
[26] E. Timmermans, P. Tommasini, M. Hussein, and A. Kerman, Phys. Rep. **315**, 199 (1999).

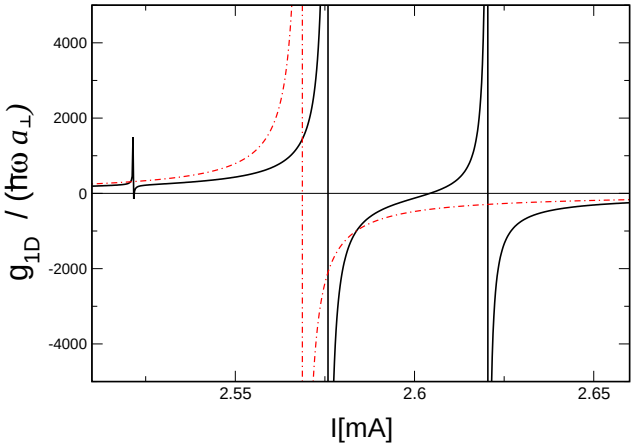

FIG. 3: (Color online) The solid curve gives $g_{1\mathrm{D}}$ as function of I for the potential (1) via numerical solution of Eq. (11) for $d \simeq 13$ and $\chi = 0.067$. The corresponding parabolic prediction for the same ω is shown as dashed curve.